Institution of Engineers, Australia, National Conference Publication
No.73/5 ,pp.77-82

Analysis and Design of Cubic Liquid Containers

By
B. Aalami, Ph.D., D.I.C.
Associate Professor of Structural Mechanics, Arya-Mehr University of Technology, Tehran, Iran

Conference on Stress and Strain in Engineering, Brisbane (Australia), 1973
Institution of Engineers, Australia, National Conference Publication, No.73/5

SUMMARY. Based on the elastic large deflection theory of plates, a design method is presented for cubic liquid containers made of thin flat sheets. The container side panels are idealised as square plates under hydrostatic pressure. The method accounts for both the membrane and bending stresses as well as their interaction. The characteristic features of the large deflection behaviour of container plate components are described. A set of large deflection data is given for the design of side panels on the basis of deflection control and first surface yield. Compared to the current design practice, the proposed method is more accurate, logical and weight saving. A numerical example illustrates the method and the use of design data presented.

1 INTRODUCTION

In a recent reference (Ref. 1) it is shown that for liquid containers made up of thin metal sheets, where the overall dimensions are large relative to the plate thickness, the conventional design procedures (Ref. 2) are unduly conservative. It is further demonstrated that a large deflection analysis can be effectively formulated and utilised for a more exact and economical design of thin plate components.

Large deflection theory accounts for the development of membrane stresses in thin plates due to out of plane deflections and also allows for their interaction with bending stresses. In the small deflection of plates only bending stresses are considered.

The current design practice (Ref. 2) in its simplest form consideres the container sides as parallel beam strips spanning horizontally between the sides or vertically between the container bottom and the top edge-beam. In the more refined practice the biaxial plate action of the sides is accounted for by using the small deflection theory of plates. Herein, a large deflection procedure is outlined for the stress analysis and design of side plates of cubic liquid containers with or without edge-beams at the top. A brief description illustrates the characteristic features of large deflections, leading to the design method with numerical examples and comparisons. The work is based on the large deflection analysis of plates developed by the author (Ref. 3) and applied successfully to other important thin plate problems (Ref. 4,5). The proposed design procedure rests on control of deflections and the first surface yield.

In the general case of the present work, the container (Fig. 1-i) is made up of flat plate components (Fig. 1-iii) rigidly connected to one another at the sides, and to the base at the bottom. The top edge may be either unsupported, or may be resting on an edge-beam, or being connected to the tank top as in the case of closed containers. For the analysis and design, the side plates are considered each under the action of a linearly varying pressure (Fig. 1-ii). The procedure and the results are general and are equally valid for partitions and bulkheads under similar loading and boundary conditions.

The boundary conditions at the edges are due to both bending and membrane actions. For bending, the conditions are as expressed in Fig. 1-iii. For membrane action, membrane shear stresses are taken as zero on the sides (due to symmetry) and at the bottom. The membrane normal stresses on the side edges are not considered due to their negligible magnitudes compared to other stresses developed in the plate. At base, the edge is assumed to remain

NOTATION

D=flexural stiffness of plate;
E=Young's modulus of elasticity;
f= Airy's stress function;
h=plate thickness;
I=edge-beam moment of inertia;
$K=k\ell_x^3/D$;
k=stiffness of elastic spring support at the top edge, equal to force per unit length of support to cause unit deflection;
ℓ=plate panel sides;
p=top edge reaction per unit length;
$Q_o=\ell_x^4\, q_o/(h^4E)$;
q_o=max intensity of hydrostatic pressure;
W=w/h;
w=plate's out of plane deflection;
x,y=rectangular coordinates;
DR=deflection reduction factor for large deflections;
ν=Poisson's ratio;
σ=normal stress;
τ=shear stress.

Superscripts.
$(\bar{\ })$=non-dimensional stresses given by $\bar{\sigma} = \ell_x^2\sigma/(h^2E)$;
(')=large deflection reduction coefficients;
(*)=large deflection reduction coefficients referring to bending stresses at plate centre.

Subscripts.
1,2,3..=refer to locations on plate shown in Fig. 1-iv;
b=bending;
e=equivalent stress;
m=membrane;
x,y= coordinate directions.

straight. The edge-beam is considered to act as a direct support to the top edge. Its interaction with the side panels is not accounted for.

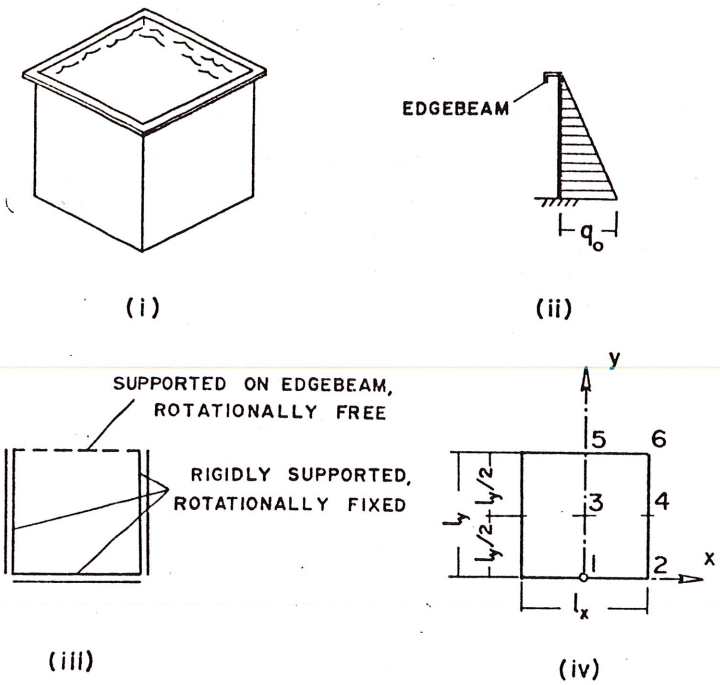

Fig. 1 (i) Cubic liquid container, (ii) presuure distribution, (iii) flexural boundary conditions of the container sides, (iv) numbering of the locations to which deflections and stresses refer.

2 ANALYSIS

(a) Formulation

There are several recently developed methods for the effective and accurate analysis of large deflection behaviour of flat plates (Ref. 5). The method used herein starts with the well established von Karman's differential equations (Ref. 6).

$$(w_{,xxxx}+2w_{,xxyy}+w_{,yyyy}) - (f_{,yy}w_{,xx}-f_{,xy}w_{,xy}+f_{,xx}w_{,yy})=q/D \quad (1)$$

$$(f_{,xxxx}+2f_{,xxyy}+f_{,yyyy}) = Eh[(w_{,xy})^2-w_{,xx}w_{,yy}] \quad (2)$$

The equations are expressed in terms of plate deflection w and Airy's stress function f, such that

$$\sigma_{xm}h=f_{,yy},\ \sigma_{ym}h=f_{,xx},\ \tau_m h = -f_{,xy} \quad (3)$$

where a comma followed by subscripts represents partial differentiation in turn with respect of each subscript variable. All other quantities related to bending and membrane actions of the loaded plate may be derived from w and f.

Due to symmetry of the problem only one half the plate need be considered, for which the relating boundary conditions are:

at $x = \ell_x/2$ $w = 0$ (4)

$w_{,x} = 0$ (5)

$\sigma_{xm}h = f_{,yy} = 0$ (6)

$\tau_m h = -f_{,xy} = 0$ (7)

at $y = 0$ $w = 0$ (Eq.4)

$w_{,y} = 0$ (8)

$-f_{,xy} = 0$ (Eq. 7)

edge remains straight with zero extensional displacement in y-deirection. This boundary condition may be achieved by imposing symmetry conditions for f function about y-y axis (Ref. 1), which on account of the boundary condition of the other edges and the equilibrium considerations, it results in zero average normal membrane stress. At x = ly, the edge is resting on a continuous elastic support of uniform stiffness, such that at each point, the out-of-plane deflection of the edge is proportional to support reaction. The support is thus represented by a continuous elastic spring with stiffness k. Further on, in describing the edge-beam design, the stiffness k of the substitute spring is related to the flexural stiffness EI of the beam. The continuous elastic spring assumption is adopted here for its relative simplicity in formulation and yet its good accuracy in representing the action of an edge-beam. Thus

$$D\,[w_{,yyy}+(2-\nu)\,w_{,xxy}] = kw \quad (9)$$

also

$$(w_{,yy}+\nu w_{,xx}) = 0 \quad (10)$$

$$\sigma_{ym}h = f_{,xx} = 0 \quad (11)$$

membrane shear stress is zero, (Eq. 7).

(b) Solution

The governing equations 1 and 2 together with the boundary contitions are solved using central finite difference approximations and a direct iterative solution technique as outlined in (Ref. 3). The plate is subdivided into a suitably graded 12 x 10 orthogonal mesh. The load is increased in 10 increments to its final value of $Q_o = 200$. The iterations are continued till the solutions obtained are within 0.5% of the values obtainable from the adopted procedure. The absolute accuracy of the solution obtained is shown (Ref. 1) tc be good.

3 RESULTS AND BEHAVIOUR

For side plates of cubic containers with the aforementioned boundary conditions non-dimensional solutions are presented in Tables I and II and Figures 2-6. Six values of elastic restraint are considered for the top edge which cover the range of rigid support (K=∞) to no support (K=0). In each case small deflection (linear) solutions together with their large deflection reduction factors (DR for deflection reduction, and SR for stress reduction) are given for central deflection W_3, deflection at mid-point of the top edge W_5 and a complete description of the biaxial state of stress at locations 1,3,4 and 5 as shown in Figure 1-v.

For simplicity in application and a rapid assessment of the relative magnitudes of stresses in each case and at each point, the numerical results in Tables I and II are related by means of reduction factors to the more familiar small deflection (linear) solutions in the following manner.

For small deflection behaviour:

$$W = w/h = W'\,Q_o, \quad (12)$$

from which

$$w = (\ell_x^4 q_o/h^3 E).\ W \quad (13)$$

W' is given on the "linear" row of each case. For more details see the numerical example. For

bending stresses the values given refer to the outside extreme fiber with tension being shown positive.

$$\bar{\sigma}_b = (\ell_x^2 \sigma_b / h^2 E) = \sigma_b' Q_o \quad (14)$$

from which

$$\sigma_b = (\ell_x^2 q_o / h^2).\sigma_b' \quad (15)$$

For large deflection behaviour:

$$W = w/h = DR.W' Q_o \quad (16)$$

where DRs are the deflection reduction factors given in Tables I and II. For example for K = 0 and Q_o = 160 from Table II DR_3 = 0.897,

$W_3' = 9.072 \times 10^{-3}$, hence

$w_3 = (0.897 \times 160 \times 9.072 \times 10^{-3})\, h = 1.3h$

Bending stresses are given by

$$\bar{\sigma}_b = (\ell_x^2 \sigma_b / h^2 E) = SR_b.\sigma_b' Q_o \quad (17)$$

For example, for the preceding case the magnitude of bending stress at centre in x-direction is

$$\sigma_{bx3} = (0.834 \times 160 \times 8.35 \times 10^{-2})(h^2 E/\ell_x^2)$$
$$= 11.1\ (h^2 E/\ell_x^2)$$

which being positive, is tensile on the outside surface. Membrane stresses are expressed in terms of the small deflection bending stresses at the same location and in the same direction by means of the membrane reduction factors (SR_m) in the following manner

$$\bar{\sigma}_m = (\ell_x^2 \sigma_m / h^2 E) = SR_m.\sigma_b' Q_o \quad (18)$$

For example, at plate centre and in x-direction of the previously mentioned plate SR_{mx3}=0.093 from Table II

$$\sigma_{mx3} = (0.093 \times 160 \times 8.35 \times 10^{-2})(h^2 E/\ell_x^2)$$
$$= 1.24\ (h^2 E/\ell_x^2)$$

It follows that for total surface stress, the corresponding bending and membrane reduction factors may be simply added together.

$$\sigma = \sigma_b + \sigma_m \quad (19)$$

$$\sigma = [SR_b + SR_m]\ (h^2 E/\ell_x^2)\ Q_o \sigma_b' \quad (20)$$

It is possible that at certain locations with zero bending stresses, membrane stresses develop due to large deflections, such as σ_{mx5} for K=∞. In such a case the membrane stress can no longer be related to the bending stress at the same point. The procedure adopted is to express these stresses as ratios of the small deflection bending stresses at plate centre and in the same direction.

The general large deflection behaviour of container side plates is illustrated in Figures 2 to 6. Figure 2 shows the central deflection and the midpoint deflection of the top edge for various edge-beam stiffnesses and transverse pressure ratios. The deflection profiles along the longitudinal centre line (y-axis) are shown in Figure 3 for the maximum value of transverse pressure considered (Q_o = 200).

For maximum loading, the distributions of bending stresses σ_{by} along the longitudinal centre line, and stresses σ_{bx} along y= $\ell_y/2$ are given in Figure 4 for both K=0 and K=∞. It is noteworthy that bending stresses are not sensitive to the edge-beam stiffness, especially in the region of their maximums.

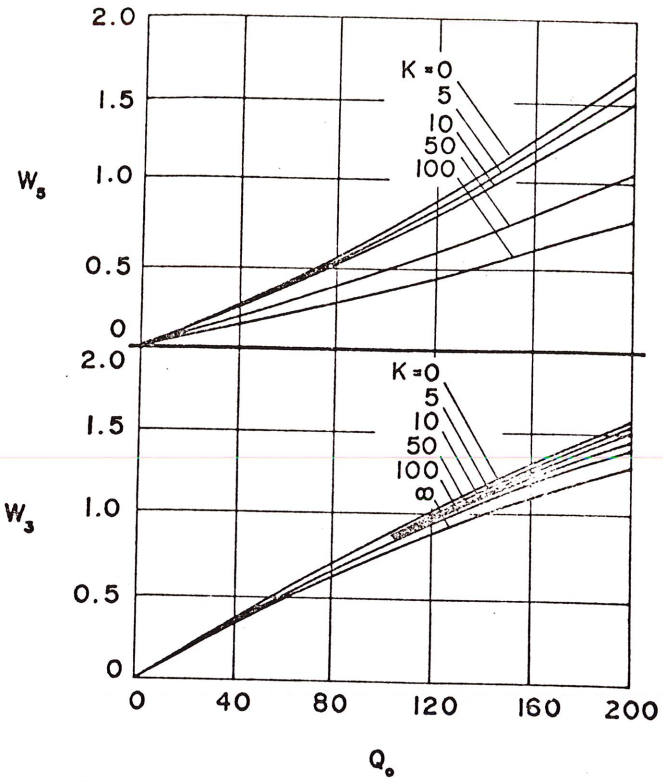

Fig. 2 Variations of central deflection (W_3), and mid-point deflection of the top edge (W_5) with the transverse pressure ratio Q_o.

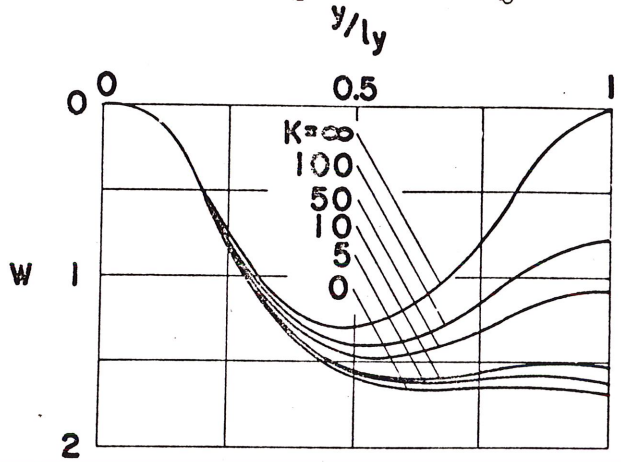

Fig. 3 Deflection profiles along y-axis for maximum loading (Q_o=200)

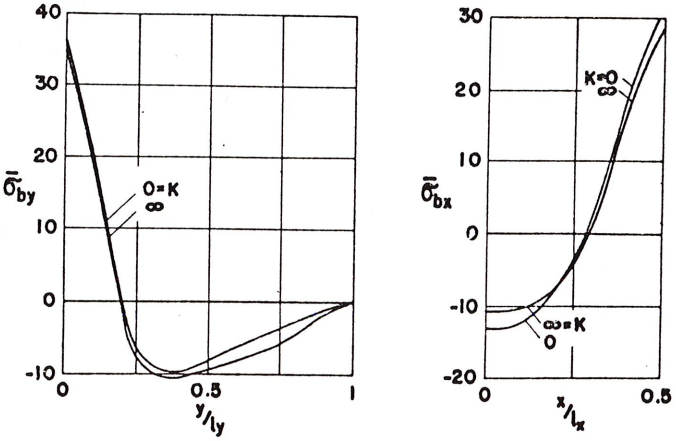

Fig. 4 Distributions of bending stresses (i) along y-axis, and (ii) along the line y=$\ell_y/2$ for maximum loading (Q_o = 200)

Figure 5 shows the distributions of membrane stresses across the boundaries and the centre lines of the plate for maximum loading considered. The

highest equivalent surface stress, based on von Mises yield criterion, occurs in all the cases considered at the midpoint of the bottom edge (x=0, y=0) on the inside surface. The second highest stressed location is the outside surface of the same point. The variation of the highest equivalent stress with the transverse pressure ratio is shown in Figure 6. The equivalent stress expression is

$$\bar{\sigma}_e = (\bar{\sigma}_x^2 + \bar{\sigma}_y^2 - \bar{\sigma}_x \bar{\sigma}_y)^{\frac{1}{2}} \qquad (21)$$

in which stresses refer to the surface, and are the sum of the bending and membrane components. Note that shearing stresses are zero at points 1,3,4,5 and 6. For comparison, the equivalent surface stress at centre (outside surface) is also shown in the same Figure.

4 DESIGN AND NUMERICAL EXAMPLES

(a) Design Considerations

(i) Plate design

For a given overall dimension (ℓ_x) of a container and the liquid density, the plate thickness (h) is determined on the basis of limitations imposed on maximum stress to avoid local yielding and control of deflections. Design curves based on these two criteria are given in Figs. 2 and 6.

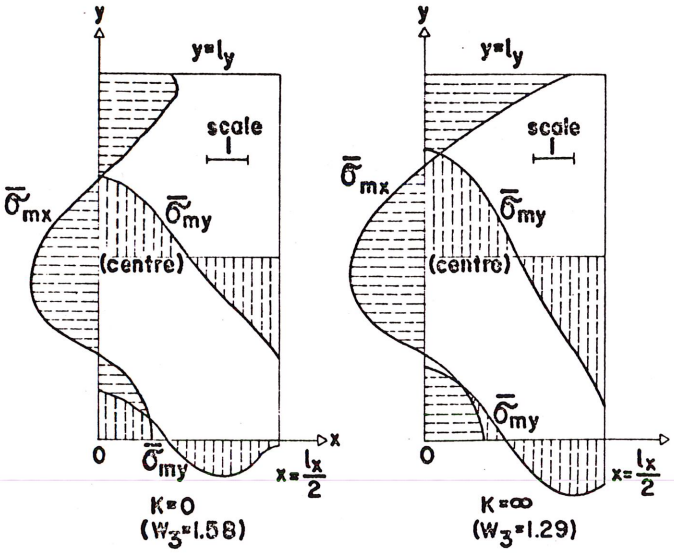

Fig. 5 Distributions of membrane stresses along the boundaries and the centre lines for maximum loading (Q_o = 200)

From the results presented and their discussions is it concluded that the maximum surface stress is not sensitive to the stiffness of the edge-beam. The plate thickness may, therefore, be determined with a good accuracy for stress limitation independent of the edge-beam design and stiffness.

To illustrate the use of the design data offered and their comparison with one other current method, consider an open container (K = 0) with the following geometrical and material characteristics: $\ell_x=\ell_y=200$cm, h=1cm, $E=2.1\times10^6$ kg/cm^2, (2.06×10^5 N/mm^2), $\nu=0.3$.

$$q_o = 0.2 \text{ kg/cm}^2, \quad (1.96\times10^{-2} \text{ N/mm}^2)$$

$$\text{hence } Q_o = \frac{\ell_x^4 q_o}{Eh^4} = \frac{200^4 \times 0.2}{2.1\times10^6 \times 1^4} = 152.4$$

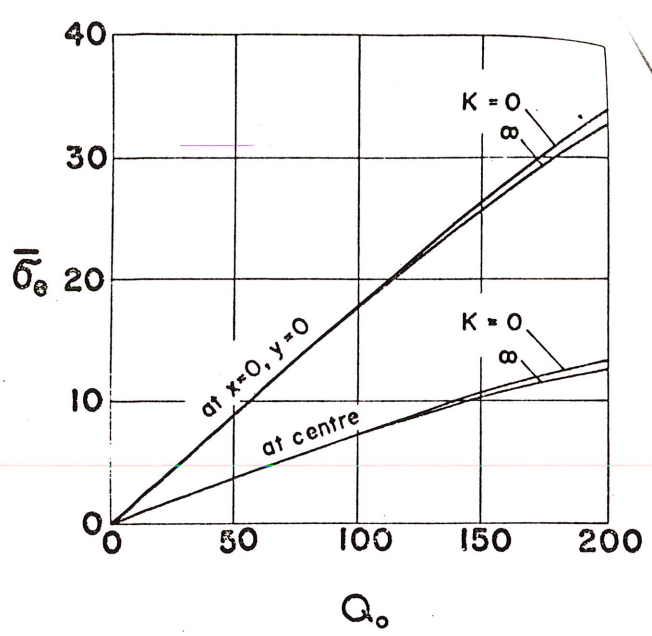

Fig. 6 Variations of maximum equivalent surface stress with transverse pressure ratio Q_o.

From Fig. 6 $\bar{\sigma}_e = 26.6$

$$\sigma_e = (h^2E/\ell_x^2)\bar{\sigma}_e = \frac{1^2 \times 2.1\times10^6 \times 26.6}{200^2}$$

$$= 1395 \text{ kg/cm}^2, \ (137 \text{ N/mm}^2)$$

The corresponding stress from Section 6.5 of (Ref. 2) is 1600 kg/cm^2. It should be noted that due to non-linear nature of the large deflection solutions the percentage difference between the two stresses is not the same for all container dimensions. From Fig. 2

$$w_3 = h''_3 = 1\times1.25 = 1.25\text{cm}$$

Deflection from (Ref. 2) is 6.10cm. This high valve is probably due to errors in preparation of design data in (Ref. 2). Reference 6 gives a small deflection w_3 = 1.72cm which agrees well with the large deflection 1.25cm of the present analysis.

(ii) Edge-beam design

The edge-beam should be selected on account of two requirements. Firstly it should be sufficiently stiff in flexure in order to reduce the top edge deflection (w_5) to the level considered satisfactory by the designer (see Fig.2) Secondly, it should withstand, with the required safety margin, the stresses set up as a result of its bending in resisting the reaction of the top edge.

The flexural stiffness of the edge-beam is related to the coefficient of elastic support K using the following simplifying argument which leads to an accurate approximation. The reaction (p_x) along the edge-beam, which is taken to be clamped at the corners is assumed to be

$$p_x = p_{max} \ [1-\cos(2\pi x/\ell)] \qquad (22)$$

Form simple beam theory the deflection profile of the edge-beam is as shown in Fig. 7, together with the small deflection and maximum large deflection profiles for K=100. On account of the close agreement between the approximated profile and the actual deflections, together with the fact that the approximated deflection along the beam at every

point is closely proportional to the reaction at that point, the edge-beam may be considered to act as a series of elastic springs of uniform stiffness. From simple beam theory the stiffness of the substitute spring is

$$k = \frac{p_{max}}{w_{max}} = \frac{514.5\ EI}{\ell_x^4} \qquad (23)$$

which may be expressed as follows.

$$K = \frac{k\ell_x^3}{D} = \frac{514.5\ EI}{\ell_x^4} = \left(\frac{5618}{\ell_x h^3}\right) I \qquad (24)$$

From which the required moment of inertia of the edge-beam for K=100 is given by

$$I = \left(\frac{200x1^3}{5618}\right) K = 3.56\ cm^4$$

For the resistance of edge-beam in flexure, the total force acting on it, and its resulting bending moments can be readily evaluated from the reaction distribution (Eq. 22) using simple beam theory. The calculated quantities may, for convenience in design and use of data presented, be related to the edge-beam substitute stiffness K and deflection at midpoint of top edge W_5 using Eqs. 23 and 24. The relationships obtained simplify to

$$\text{total reaction} = 0.0457\ (Eh^4K/\ell_x^2)\ W_5 \qquad (25)$$

TABLE I

Hydrostatically loaded square plates with edge-beam stiffnesses K = ∞, 100, 50.
Small deflection coefficients and large deflection reduction factors for deflections and stresses.

K	Q_o	W_3	W_5	σ_{by1}	σ_{bx3}	σ_{by3}	σ_{bx4}	σ_{bx5}	σ_{mx1}	σ_{my1}	σ_{mx3}	σ_{my3}	σ_{my4}	σ_{mx5} or σ^*_{mx5}
∞	Linear 1	8.337 x10^{-3}	0	19.7 x10^{-2}	7.90 x10^{-2}	7.03 x10^{-2}	16.8 x10^{-2}	0	0	0	0	0	0	0
	20	0.996	1	-0.997	0.992	0.992	-0.997	0	-0.022	0.007	0.023	0.035	-0.060	-0.037
	40	0.980	1	-0.990	0.972	0.970	-0.988	0	-0.043	0.014	0.043	0.067	-0.118	-0.071
	80	0.934	1	-0.966	0.904	0.900	-0.959	0	-0.077	0.026	0.076	0.119	-0.213	-0.130
	120	0.879	1	-0.937	0.826	0.820	-0.924	0	-0.101	0.036	0.098	0.155	-0.284	-0.174
	160	0.825	1	-0.907	0.751	0.743	-0.889	0	-0.117	0.042	0.110	0.178	-0.335	-0.206
	200	0.775	1	-0.879	0.684	0.676	-0.856	0	-0.128	0.047	0.118	0.193	-0.373	-0.230
100	Linear 1	8.719 x10^{-3}	3.292 x10^{-3}	19.9 x10^{-2}	8.14 x10^{-2}	6.63 x10^{-2}	17.2 x10^{-2}	3.03 x10^{-2}	0	0	0	0	0	0
	20	0.997	1.002	-0.998	0.992	0.995	-0.997	1.00	-0.021	0.007	0.021	0.033	-0.052	-0.115
	40	0.983	1.010	-0.991	0.974	0.970	-0.989	1.01	-0.041	0.013	0.041	0.065	-0.105	-0.201
	80	0.943	1.037	-0.970	.915	0.899	-0.963	1.03	-0.075	0.024	0.072	0.117	-0.193	-0.348
	120	0.895	1.076	-0.944	0.847	0.815	-0.931	1.06	-0.099	0.032	0.092	0.153	-0.258	-0.459
	160	0.849	1.120	-0.918	0.783	0.736	-0.899	1.10	-0.116	0.038	0.104	0.176	-0.303	-0.539
	200	0.808	1.171	-0.894	0.725	0.666	-0.870	1.15	-0.127	0.042	0.111	0.191	-0.334	-0.598
50	Linear 1	8.837 x10^{-3}	4.339 x10^{-3}	19.9 x10^{-2}	8.21 x10^{-2}	6.50 x10^{-2}	17.3 x10^{-2}	3.87 x10^{-2}	0	0	0	0	0	0
	20	0.996	1.003	-0.998	0.994	0.992	-0.997	1.00	-0.020	0.006	0.021	0.032	-0.049	-0.091
	40	0.984	1.014	-0.992	0.977	0.970	-0.990	1.01	-0.040	0.012	0.040	0.063	-0.099	-0.153
	80	0.948	1.051	-0.972	0.921	0.899	-0.966	1.05	-0.073	0.022	0.070	0.115	-0.183	-0.259
	120	0.904	1.102	-0.947	0.857	0.815	-0.936	1.10	-0.097	0.030	0.090	0.150	-0.243	-0.333
	160	0.863	1.164	-0.923	0.796	0.735	-0.907	1.16	-0.114	0.036	0.101	0.172	-0.283	-0.387
	200	0.828	1.234	-0.901	0.745	0.664	-0.880	1.24	-0.125	0.039	0.107	0.185	-0.308	-0.418

TABLE II

Hydrostatically loaded square plates with edge-beam stiffnesses K = 10, 0.
Small deflection coefficients and large deflection reduction factors for deflections and stresses.

K	Q_o	W_3	W_5	σ_{by1}	σ_{bx3}	σ_{by3}	σ_{bx4}	σ_{bx5}	σ_{mx1}	σ_{my1}	σ_{mx3}	σ_{my3}	σ_{my4}	σ_{mx5}
10	Linear 1	9.009 x10^{-3}	5.848 x10^{-3}	19.9 x10^{-2}	8.31 x10^{-2}	6.31 x10^{-2}	17.5 x10^{-2}	5.08 x10^{-2}	0	0	0	0	0	0
	20	0.999	1.009	-0.998	0.995	0.992	-0.999	1.01	-0.019	0.006	0.020	0.030	-0.043	-0.068
	40	0.988	1.022	-0.993	0.980	0.970	-0.992	1.02	-0.039	0.011	0.038	0.060	-0.089	-0.108
	80	0.956	1.069	-0.975	0.931	0.899	-0.970	1.07	-0.071	0.020	0.066	0.109	-0.164	-0.173
	120	0.919	1.136	-0.953	0.874	0.814	-0.944	1.14	-0.094	0.027	0.085	0.142	-0.216	-0.213
	160	0.887	1.216	-0.932	0.823	0.734	-0.920	1.22	-0.110	0.032	0.095	0.160	-0.245	-0.230
	200	0.861	1.305	-0.914	0.782	0.664	-0.900	1.32	-0.121	0.034	0.100	0.170	-0.258	-0.228
0	Linear 1	9.072 x10^{-3}	6.410 x10^{-3}	20.0 x10^{-2}	8.35 x10^{-2}	6.24 x10^{-2}	17.6 x10^{-2}	5.52 x10^{-2}	0	0	0	0	0	0
	20	0.997	1.006	-0.998	0.995	0.992	-0.998	1.01	-0.019	0.005	0.019	0.029	-0.041	-0.062
	40	0.989	1.026	-0.993	0.981	0.970	-0.992	1.03	-0.038	0.011	0.037	0.059	-0.085	-0.096
	80	0.959	1.076	-0.976	0.934	0.899	-0.974	1.08	-0.069	0.020	0.065	0.107	-0.156	-0.148
	120	0.926	1.148	-0.955	0.881	0.814	-0.948	1.15	-0.092	0.026	0.083	0.138	-0.203	-0.176
	160	0.897	1.231	-0.936	0.834	0.734	-0.927	1.24	-0.108	0.030	0.093	0.155	-0.228	-0.182
	200	0.875	1.321	-0.919	0.797	0.665	-0.907	1.34	-0.119	0.032	0.098	0.163	-0.236	-0.170

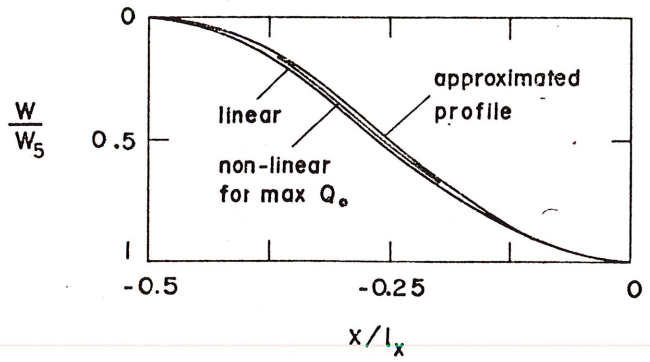

Fig. 7 Deflection profiles along the top edge for K=100

Maximum moment occurs at the corners

$$M_{max} = -0.00497\ (Eh^4 K/\ell_x)\ W_5 \qquad (26)$$

At midspan (midpoint of top edge)

$$M = 0.00307\ (Eh^4 K/\ell_x)\ W_5 \qquad (27)$$

(b) Numerical Example

The following illustrates the use of the small deflection and large deflection numerical coefficients given in Tables I and II.

Consider the same container used in the preceding design example for which the relating numerical coefficients are given at the bottom half of Table II. Deflection at centre from small deflection theory

$$W_3 = Q_o W'_3 = 152.4 \times 9.072 \times 10^{-3} = 1.38$$

$$w_3 = hW_3 = 1 \times 1.38 = 1.38 \text{ cm}$$

from large deflection theory

$$W_3 = DR.W'_3 Q_o = 1.25$$

$$w_3 = 1.25 \text{ cm}$$

Stresses at centre, in x-direction and from small deflection theory

$$\bar{\sigma}_{bx3} = Q_o \sigma'_{bx3} = 12.76$$

$$\sigma_{bx3} = (Eh^2/\ell_x^2)\bar{\sigma}_{bx3} = 670 \text{ kg/cm}^2, (66 \text{ N/mm}^2)$$

from large deflection theory

$$\bar{\sigma}_{bx3} = SR_{bx3}.\sigma'_{bx3} Q_o = 10.72$$

$$\sigma_{bx3} = (Eh^2/\ell_x^2)\ \bar{\sigma}_{bx3} = 563 \text{ kg/cm}^2, (55 \text{N/mm}^2)$$

for membrane action

$$\bar{\sigma}_{mx3} = SR_{mx3}\ .\bar{\sigma}_{bx3}\ Q_o = 1.16$$

$$\sigma_{mx3} = 61 \text{ kg/cm}^2, (6 \text{ N/mm}^2)$$

5 CONCLUSIONS

The elastic large deflection theory of plates is used to study the behaviour of flat side panels of thin liquid containers. The rate of charge of deflection and bending stresses are found to reduce at plate centre, and to increase at the midpoint of the top edge due to the action of large deflections. The changes in bending stresses together with the development of membrane stresses result in a distribution of surface stress which is significantly different from that given by the small deflection analysis. The use of the proposed large deflection design procedure and data are improvements in the means of estimating the side plate deflections and stresses, upon which the current design practice is based.

The scope of the present data may be increased by provision of similar curves and tables for rectangular plates and for plates under partial hydrostatic loading.

6 ACKNOWLEDGMENT

The author is grateful to Miss C. Grigorian for her extra care and patience in typing this manuscript.

7 REFERENCES

1. AALAMI, B. - Large Deflection of Plates under Hydrostatic Pressure, With Special Reference to Liquid Containers. Journal of Ship Research, No. 4, Vol. 16, Dec., 1972.

2. BLODGETT, O.W. - Design of Welded Structures, James Lincoln Foundation, 1967.

3. AALAMI, B. and CHAPMAN, J.C. - Large Deflection Behaviour of Orthotropic Plates Under Transverse and In-Plane Loads. Proc. of The Institution of Civil Engineers, Vol. 42, March, 1969, pp. 347-264.

4. AALAMI, B. and CHAPMAN, J.C. - Large Deflection Behaviour of Ship Plate Panels Under Normal Pressure and In-Plane Loading. Quarterly Trans. of The Royal Institution of Naval Architects, Vol. 114, April, 1972, pp. 155-181.

5. AALAMI, B. - Large Deflection of Elastic plates Under Patch Loading. Journal of The Structural Division, ASCE, Vol. 98, No. ST11, Nov., 1972, pp. 2567-2586.

6. TIMOSHENKO, S. and WOINOWSKI-KRIEGER - Theory of Plates and Shells. New York, McGraw Hill Book Co., Inc., 1959, pp. 580.

TABLE III

Hydrostatically loaded rectangular plates with K=0 (topedge free). small deflection coefficients and large deflection reduction factors for deflections and stresses.

ℓ_y/ℓ_x	Q_o	W'_3	σ'_{by1}	σ'_{bx3}	σ'_{by3}	σ'_{bx4}	σ'_{mx1}	σ'_{my1}	σ'_{mx3}	σ'_{my3}	σ'_{my4}	σ^*_{mx5}	σ_{e1}	σ_{e3}
0.5	Linear	4.237												
	1	$X10^{-2}$	1.397	0.683	0.355	1.374	0.0	0.0	0.0	0.0	0.0	0.0	1.26	0.6
	20	0.993	-0.997	0.991	0.989	-0.995	-0.061	0.014	0.020	0.123	-0.141	-0.013	25.2	12.0
	40	0.974	-0.987	0.966	0.960	-0.981	-0.114	0.027	0.037	0.232	-0.268	-0.027	50.9	23.9
	80	0.919	-0.959	0.895	0.875	-0.941	-0.198	0.049	0.061	0.399	-0.467	-0.059	102.0	46.3
	120	0.860	-0.928	0.820	0.789	-0.896	-0.252	0.065	0.072	0.507	-0.601	-0.093	152.3	66.0
	160	0.805	-0.898	0.752	0.716	-0.854	-0.288	0.078	0.077	0.576	-0.692	-0.125	200.0	83.3
	200	0.758	-0.870	0.695	0.655	-0.818	-0.312	0.087	0.079	0.622	-0.754	-0.156	247.0	99.0
1.5	Linear	1.155												
	1	$X10^{-2}$	0.826	0.226	0.349	0.556	0.0	0.0	0.0	0.0	0.0	0.0	0.735	0.312
	20	0.999	-1.000	0.999	0.999	-1.000	-0.009	0.006	0.026	0.015	-0.035	-0.062	14.7	6.23
	40	0.997	-0.998	0.994	0.995	-0.999	-0.017	0.013	0.051	0.030	-0.069	-0.122	29.7	12.6
	80	0.987	-0.992	0.978	0.982	-0.995	-0.033	0.025	0.101	0.058	-0.135	-0.239	60.0	25.6
	120	0.972	-0.983	0.953	0.962	-0.989	-0.048	0.036	0.145	0.084	-0.198	-0.347	90.3	38.7
	160	0.953	-0.971	0.923	0.937	-0.982	-0.061	0.046	0.185	0.106	-0.256	-0.444	120.0	51.6
	200	0.932	-0.958	0.889	0.909	-0.973	-0.072	0.055	0.219	0.125	-0.309	-0.528	150.0	64.0

σ_{e1} liquid side surface

σ_{e3} free side surface

TABLE IV

Hydrostatically loaded rectangular plates with K=∞ (top edge on rigid supports). Small deflection coefficients and large deflection reduction factors for deflections and stresses.

ℓ_y/ℓ_x	Q_o	W'_3	W'_5	σ'_{by1}	σ'_{bx3}	σ'_{by3}	σ'_{bx4}	σ'_{bx5}	σ'_{mx1}	σ'_{my1}	σ'_{mx3}	σ'_{my3}	σ'_{my4}	σ'_{mx5}	σ_{e1}	σ_{e3}
0.5	Linear 1	1.700 $X10^{-2}$	2.335 $X10^{-2}$	0.945	0.288	0.266	0.671	0.336	0.0	0.0	0.0	0.0	0.0	0.0	0.840	0.279
	20	1.003	1.008	-1.001	1.003	0.998	-1.002	1.008	-0.004	-0.002	0.009	-0.004	0.061	-0.092	16.7	5.57
	40	1.006	1.016	-1.002	1.004	0.995	-1.004	1.018	-0.017	-0.000	0.026	0.010	0.066	-0.114	33.7	11.3
	80	1.010	1.036	-1.003	1.002	0.981	-1.007	1.040	-0.043	0.003	0.059	0.036	0.079	-0.154	67.8	23.1
	120	1.012	1.057	-1.003	0.997	0.960	-1.009	1.064	-0.067	0.005	0.088	0.059	0.100	-0.184	102.0	35.2
	160	1.013	1.078	-1.003	0.988	0.936	-1.012	1.089	-0.091	0.007	0.114	0.078	0.129	-0.204	136.0	47.4
	200	1.014	1.099	-1.002	0.977	0.911	-1.015	1.114	-0.114	0.007	0.136	0.094	0.165	-0.214	171.0	59.5
1.5	Linear 1	4.269 $X10^{-2}$	1.351 $X10^{-2}$	1.396	0.685	0.342	1.377	0.227	0.0	0.0	0.0	0.0	0.0	0.0	1.26	0.60
	20	0.994	1.027	-0.997	0.992	0.989	-0.995	1.009	-0.059	0.014	0.019	0.116	-0.129	-0.038	25.2	12.0
	40	0.977	1.050	-0.988	0.970	0.961	-0.983	1.030	-0.111	0.026	0.035	0.219	-0.245	-0.051	50.9	23.9
	80	0.929	1.127	-0.960	0.906	0.878	-0.947	1.099	-0.192	0.047	0.057	0.375	-0.426	-0.086	102.0	46.3
	120	0.878	1.231	-0.931	0.841	0.794	-0.907	1.194	-0.245	0.062	0.068	0.471	-0.544	-0.124	152.0	66.3
	160	0.833	1.352	-0.903	0.786	0.721	-0.872	1.307	-0.279	0.073	0.072	0.529	-0.617	-0.153	200.0	84.1
	200	0.796	1.485	-0.877	0.740	0.662	-0.841	1.435	-0.301	0.080	0.073	0.561	-0.660	-0.166	247.0	100.0

σ_{e1} liquid side surface
σ_{e3} free side surface